COBEM 2021 26th International Congress of Mechanical Engineering
November 22-26, 2021, Virtual Congress, Brazil

COB-2021-1130
CORROSION FATIGUE ANALYSIS OF GRADE R4 STEEL IN SIMULATED SEAWATER

Felipe Azevedo Canut
Department of Mechanical Engineering, University of Brasília, 70910-900 Brasília, DF, Brazil.
felipe.canut@gmail.com

Alda Maria Pereira Simões
Centro de Química Estrutural, Instituto Superior Técnico, Universidade de Lisboa, Av. Rovisco Pais, 1049-001 Lisbon, Portugal.

Luis Reis
Instituto de Engenharia Mecânica, Instituto Superior Técnico, Universidade de Lisboa, Av. Rovisco Pais, 1049-001 Lisbon, Portugal.

Ivan Napoleão Bastos
Instituto Politécnico, Universidade do Estado do Rio de Janeiro, 28.625-570 Nova Friburgo, RJ, Brazil.

Edgar Nobuo Mamiya
Department of Mechanical Engineering, University of Brasília, 70910-900 Brasília, DF, Brazil.

Abstract. *Offshore structures are often submitted to severe field conditions, combining fatigue loads and corrosive marine environments, which may result in early failure and safety issues. The study is focused on the combined effect of corrosion and mechanical cyclic stresses observed on mooring chains of Floating Production Storage and Offloading (FPSO) units. Grade R4 steel, commonly used in the production of mooring chains, was studied. Corrosion-fatigue tests were performed in artificial seawater (3.5 wt% NaCl) under stress-controlled loading using a corrosion cell developed for this purpose. Fully reversed (R = -1) and tension-tension (R = 0.1) loads were applied. In-air fatigue and no-load immersion tests were also carried out for comparative purposes. The results have shown an acceleration of the failure caused by the corrosive environment when compared to the in-air fatigue. The corrosive environment also seems to have ever-increasing importance towards lower stress amplitudes on the observed corrosion-fatigue life. After the failure, the specimens were examined in a scanning electron microscope (SEM) and in a confocal microscope. The corrosion attack on the specimens' lateral surface was evaluated using the corroded area fraction as an index. The analysis has shown that the application of mechanical loads causes a greater corrosion degradation level, highlighting the synergistic nature of the corrosion-fatigue phenomenon. The morphology of the corroded surfaces also varied for different levels of fatigue loads. A high density of microcracks and pits were observed for the lower fatigue loads while large secondary cracks and few pits were identified for the higher amplitudes. Therefore, the failure of grade R4 steel in the seawater environment could be divided into two regimes: one dominated by electrochemical effects, observed in lower stress amplitude, and the other dominated by mechanical effects, for higher stress amplitude.*

Keywords: *Corrosion-Fatigue, Grade R4 Steel, FPSO, Mooring Chains.*

1. INTRODUCTION

The discovery of deep-water oil reserves with depths greater than 1500 m have created the necessity of new types of oil extracting structures, the so-called Floating Production Storage and Offloading (FPSO) units. This type of structure must stay at a fixed position for decades without dry-docking for inspection or repair. In FPSO units, the stationkeeping positioning is achieved by using mooring systems composed of several lines. Each mooring line consists of an association of steel chains and synthetic ropes. Steel chains are typically used at the top and the bottom ends of the mooring line, splash zone and trash zone, respectively. In these zones, the possibility of marine life growth due to sunlight exposure and the wear due to the contact with sea bed precludes the use of synthetic ropes.

Mooring systems are typically designed for lives that can exceed 20 years of service. During this timespan, steel chains must withstand field conditions combining corrosive marine aggressiveness and high static and dynamic loads. The protection against corrosion is usually provided by increasing the diameter of the chain links. According to the standard API-2SK (2018), the diameter of chain links situated in the splash zone or trash zone must consider an additional 0.4 mm to 1.0 mm per year of service life. Various sources of mooring line failure, such as corrosion-fatigue of the chain

links (Pérez-Mora *et al.*, 2015; Gordon *et al.*, 2014; Fontaine *et al.*, 2012; Rampi and Vargas, 2011) and Out of Plane Bending (Mamiya *et al.*, 2019; Ma *et al.*, 2013) have been identified. The failure of mooring line is a critical event that might cause high environmental and economic costs. The cost of a single line failure can be as high as £10.5M (HSE, 2006), considering a production of 250 thousand oil barrels per day (BPD).

The behaviour of offshore structural steels is strongly affected by the presence of seawater environment, and structures become susceptible to premature crack initiation and higher rates of crack propagation leading to a decrease in fatigue strength (Rampi and Vargas, 2011). The combined damage due to corrosion and cyclic loading has been observed to be greater than the damage caused by each of then acting separately (Palin-Luc *et al.*, 2010; Pérez-Mora *et al.*, 2015). There are many studies on the effect of the maritime environment on the fatigue life of mooring chain steels (Pérez-Mora *et al.*, 2015; Fontaine *et al.*, 2012; Fernández *et al.*, 2014), and on the effect of local physicochemical parameters (*e.g.*, temperature, salinity, dissolved oxygen) on the corrosion rate (Nevshupa *et al.*, 2018). Nevertheless, many aspects of the synergy between corrosion and fatigue remain open. Recently, Canut *et al.* (2019) carried out a number of corrosion-fatigue experiments on smooth specimens of grade R4 steel immersed in artificial seawater. The corrosion potential response was monitored and correlated with the degradation of the specimen. The synergistic nature of corrosion-fatigue was observed from the results for specimens without load and under cyclic load.

The aim of this work is to study the influence of the corrosive environment on the fatigue life of grade R4 steels. Corrosion-fatigue and in-air fatigue experiments with different load ratios were carried out and the observed lives were compared in order to evaluate the detrimental effects of the aggressive environment. A post-failure inspection of the specimens was performed and a quantitative analysis of the corrosion degradation due to corrosion-fatigue was carried out. The morphology of the propagation surface for the different conditions tested were also addressed.

2. METHODOLOGY

The material used in the study is the martensitic grade R4 steel. According to the International Association Classification Societies (IACS, 2016), this material must contain a minimum of 0.2% of molybdenum and its mechanical properties must satisfy the following requirements: minimum yield stress of 580 MPa, minimum tensile strength of 860 MPa, minimum elongation of 12%, and minimum reduction of area of 50%. To characterize the microstructure of the material, a specimen was grounded, polished using alumina and etched with nital 3%. The micrography of the plane perpendicular to the specimen axis is shown in the Fig. 1, in which the martensitic microstructure of material can be observed.

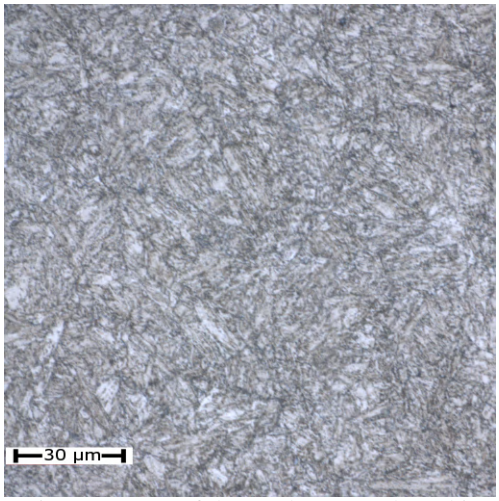

Figure 1. Microstructure of the grade R4 steel used in the study.

The steel was quenched and tempered to meet the requirements of the standard and its final properties assessed under quasi-static monotonic tensile tests were: 204 GPa Young's modulus, 0.2%-offset yield stress of 905 MPa and 957 MPa ultimate tensile strength. Cylindrical specimens with a gauge length of 12 mm and uniform diameter of 6 mm were machined from round bars. The surfaces were abraded with emery paper up to grade 1000 and then degreased with acetone and dried with air jet. The arithmetic roughness, R_a, on the specimen longitudinal axis direction was measured using a Confocal Microscope (Olympus OLS 4000 LEXT). The typical surface roughness value was $R_a = 0.07$ μm. This value is significantly lower than 0.2 μm, which is the roughness stipulated by the standard ASTM E 466 for fatigue in air tests and 0.4 μm stipulated by ASTM F 1801 for corrosion-fatigue testing of metallic implant materials. To the best of the authors' knowledge, there is not a standard concerning the surface roughness limit for corrosion-fatigue tests of steels in artificial seawater.

A corrosion cell was developed to allow *in-situ* corrosion-fatigue testing in artificial seawater (3.5 wt% NaCl solution).

The cell consists of an acrylic chamber which surrounds the working section of the specimen. The cell has two lateral accesses, which can be used to perform electrochemical measurements during the corrosion-fatigue tests. Both ends of the specimen are clamped to a servohydraulic fatigue testing machine. The solution was prepared using deionised Millipore water and pure NaCl (by Sigma–Aldrich). The schema and a picture of the corrosion-fatigue test setup are shown in Fig. 2.

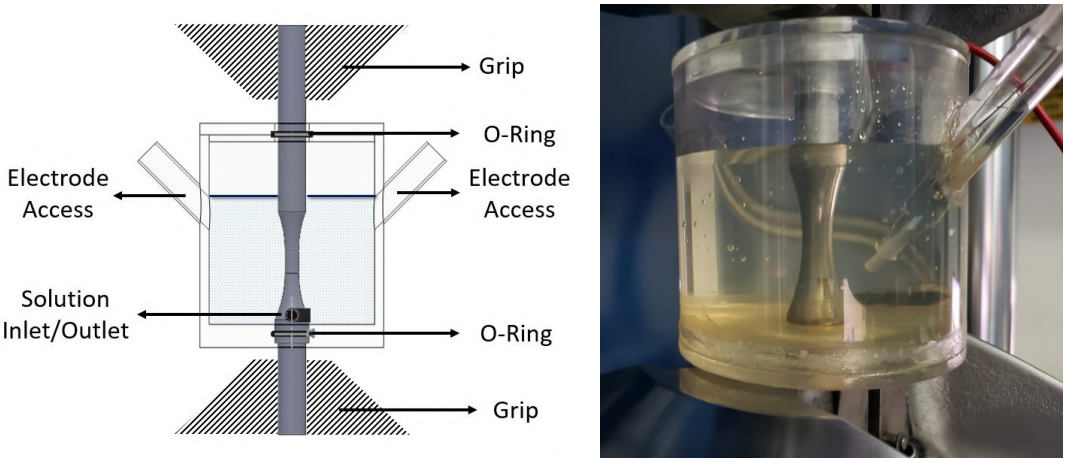

(a) (b)

Figure 2. (a) Schema and (b) corrosion cell used for the corrosion-fatigue experiments.

The corrosion-fatigue tests were performed under load control regime with sinusoidal waveform and 1.0 Hz load frequency. Fully reversed loads, $R = -1$, and tests in the presence of mean stress, $R = 0.1$, were performed. In-air fatigue tests were also performed for comparative purposes. The stop criterion for the fatigue tests was defined as the complete rupture of the specimen. Specimens that did not fail after 2 million cycles were identified as "runout". All tests were carried out at room temperature.

3. RESULTS

The fatigue curves for the tests carried out in air and in corrosive environment are shown in Fig. 3 where the arrows represent runouts. Fully reversed loads ($R = -1$) and load with mean stress ($R = 0.1$) were considered. The data reveal a significant reduction of the number of cycles to failure for the tests carried out in the corrosive environment, even for higher stress amplitudes wherein the exposure times were lower than 12 hours. The results highlight the severity of the seawater environment on the fatigue life of grade R4 steel. The corrosive environment, under spontaneous potential, also seems to have ever-increasing importance for lower stress amplitudes on the observed corrosion-fatigue life. For the same load amplitude, the presence of the mean stress causes a reduction of the number of cycles to failure. The effects of the positive load ratio are particularly important for the corrosion-fatigue experiment. In this condition, the specimen is always under traction, causing the nucleated cracks to remain open during the whole loading cycle and exposed to the corrosive environment. This phenomenon is not observed in the fully reversed tests, in which the cracks stay closed during the compressive phase of the loading cycle.

The Smith-Watson-Topper parameter (Smith *et al.*, 1970) was used to take into account the effect of mean stress on the fatigue life, as shown in Fig. 4. This parameter has been already used in corrosion-fatigue studies (Morgantini *et al.*, 2018) in the presence of mean stress and have shown good results when compared to the experimental data. The *SWT* parameter for conditions where macroscopic plasticity is not observed can be defined as:

$$SWT = \sqrt{S_a S_{max}} \tag{1}$$

where S_a is the nominal stress amplitude and S_{max} is the maximum nominal stress.

The data shown in Fig. 4 reveals that the *SWT* parameter is able to capture the mean stress effect for both environmental conditions tested. A significant reduction of the number of cycles to failure for the tests carried out in the corrosive environment for stress amplitudes lower than *SWT* = 600 MPa was observed. For a stress amplitude of *SWT* = 500 MPa the in-air fatigue life is already 20 times greater when compared to corrosion-fatigue condition. For lower stress amplitudes, the failure was only observed in the corrosion-fatigue experiments, considering a runout of 2 million cycles.

3.1 Corrosion level quantitative analysis

The corrosion-fatigue specimens were submitted to a confocal microscopic inspection after the rupture aiming to evaluate the level of corrosion degradation. The fraction of corroded area was used as a parameter. The identification

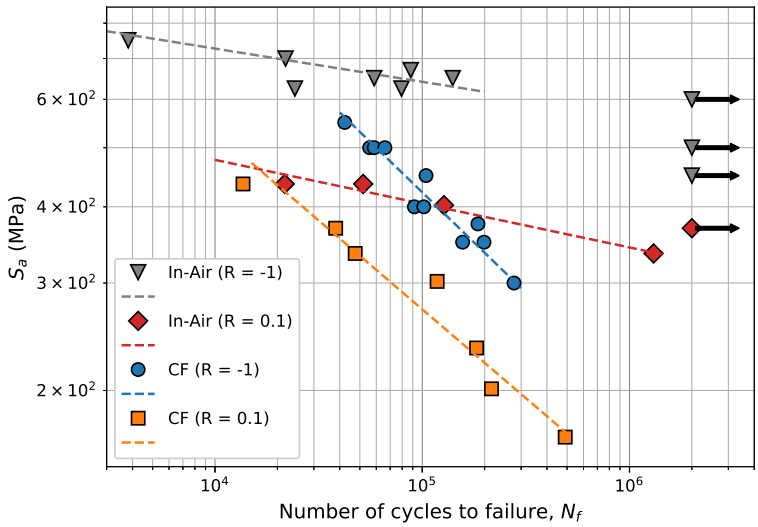

Figure 3. In-air and corrosion-fatigue (CF) curves.

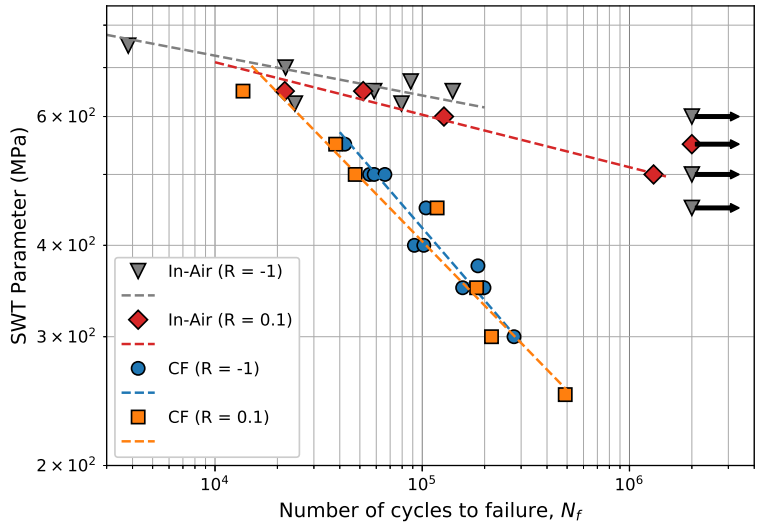

Figure 4. In-air and corrosion-fatigue (CF) curves using the *SWT* parameter.

of the corroded zones was performed automatically, using a Python script developed for this purpose. The identification processes consists of 3 stages: *i)* The image colouring is modified to greyscale (Fig. 5a). *ii)* A grey threshold is applied and the darker areas are identified as corroded regions. The total corroded area is calculated in this stage (Fig. 5b). *iii)* The identified zone are marked on the original image to validate the process (Fig. 5c). In order to obtain a better estimation of the fraction of corroded area, four images with the area of $640\ \mu$m x $640\ \mu$m were used for each load condition and the mean corroded area was calculated. The standard deviation was used as a dispersion measure.

The corrosion levels obtained for $R = -1$ and $R = 0.1$ load ratios are shown in Fig. 6a and Fig. 6b, respectively. In both conditions, it is possible to observe a positive correlation between the fraction of corroded area and the stress amplitude up to approximately 350 MPa. Above this threshold, the fraction of corroded area decreased abruptly. It is noteworthy that the duration of the immersion test, with no mechanical load applied, and the duration of the tests submitted to 350 MPa for both load ratios are quite similar, however, the fraction of the corroded area increased significantly in the presence of mechanical load. This behaviour highlights the synergistic nature of the corrosion-fatigue phenomenon.

For higher stress amplitudes, the corrosion level does not seem to be influenced by the applied mechanical load. In this condition, the immersion times are shorter due to the lower fatigue lives. Furthermore, a shorter time for crack nucleation is expected for the higher stress amplitudes. After a crack is nucleated, the anodic region shifts from the specimen's surface to the interior of the crack generating a cathodic region around the crack (Gabetta, 1982). This behaviour causes

a high corrosion rate on the interior of the crack decreasing the overall corrosion rate on the surface of the specimen.

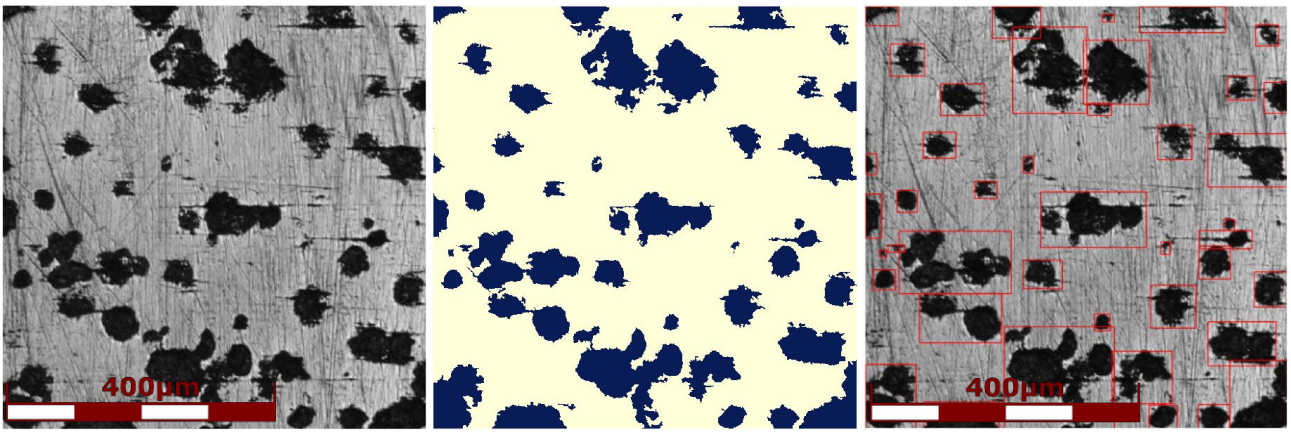

(a) (b) (c)

Figure 5. Stages (a) 1, (b) 2 and (c) 3 of the corrosion level identification process.

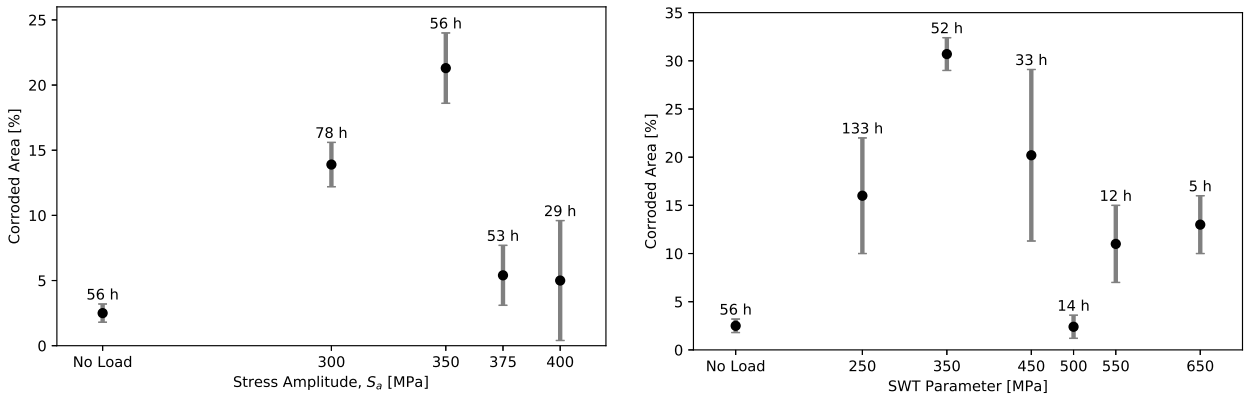

(a) (b)

Figure 6. Fraction of the corroded area for (a) $R = -1$ e (b) $R = 0.1$ load ratios.

3.2 Corrosion morphology analysis

After the rupture, the specimens were submitted to a Scanning Electron Microscope (SEM) analysis in order to evaluate the lateral surface and fractured surface morphology. This analysis was performed on the specimens under $R = 0.1$ load ratio. The absence of the compressive phase in the load cycle for this condition preserves valuable information on the propagation surface.

The lateral surface of the specimen was checked for secondary cracks and corrosion defects. The level of surface degradation varied significantly depending on the applied stress, and consequently on the immersion time. For the highest tested amplitude, $SWT = 650$ MPa, a few large cracks (more than 300 μm long) and a few corrosion pits were observed. However, for the lower tested amplitude, a great density of microcracks (shorter than 200 μm) and corrosion pits were identified. For this condition, the microcracks do not seem to be related with the stress concentrators generated by the corrosion defects.

The microcracks observed for the lower stress condition have random orientations and are not perpendicular to the applied stress which suggests that the crack nucleation occurs at the grain boundaries of the material. These regions are known to be prone to anodic dissolution (Larrosa *et al.*, 2017). Since this behaviour was identified for the specimens under low stress amplitude and a higher immersion period, it is reasonable to assume that the failure under this conditions is dominated by the electrochemical processes.

For the higher stress amplitudes, completely perpendicular cracks, with length greater than 300 μm, were identified. The immersion period for corrosion-fatigue experiments under high stress amplitudes are shorter when compared to the lower stress amplitudes (5 h for $SWT = 650$ MPa versus 137 h for $SWT = 250$ MPa). Since higher stress amplitudes tend to produce a failure morphology closer to the one observed for the in-air condition, the failure for this load level is assumed to be mechanically driven.

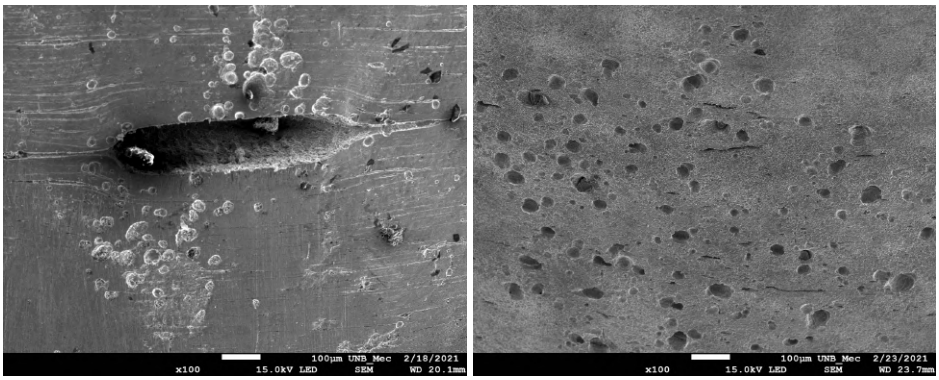

(a) (b)

Figure 7. Lateral surface of the corrosion-fatigue specimens under (a) SWT = 650 MPa and (b) SWT = 250 MPa.

The fractured surfaces for the corrosion-fatigue condition are shown in Fig. 8a and Fig. 8b, while the fractured surface for in-air condition is shown in Fig. 8c. The respective regions are shown in details in Fig. 9. From Figure 8, it is possible to observe that more severe load amplitudes generate smaller propagations zones. Perpendicular propagations planes were observed for all the conditions tested. It is also possible to identify a inclined plane in relation to the longitudinal axis after the propagation zone which is caused by the monotonic failure of the material due to shear stress.

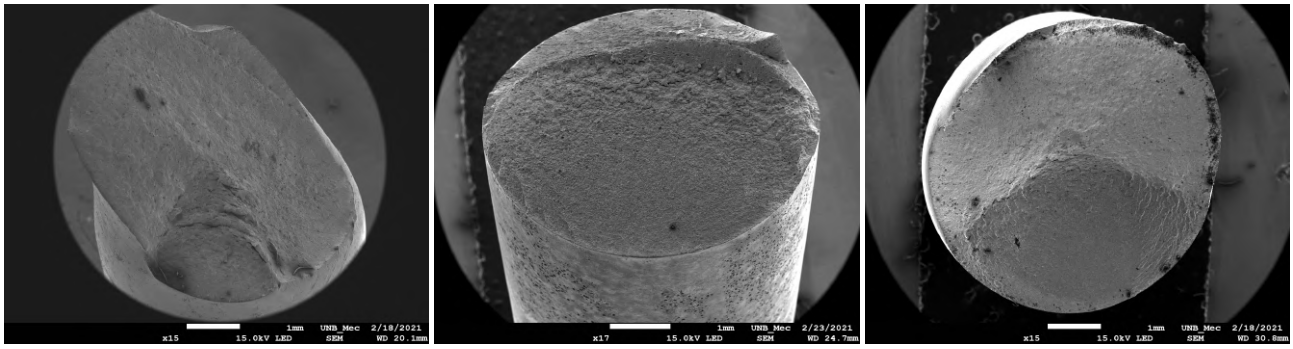

(a) (b) (c)

Figure 8. Corrosion-fatigue specimens under load amplitude of: (a) SWT = 650 MPa and (b) SWT = 250 MPa. In-air fatigue specimen under (c) SWT = 500 MPa.

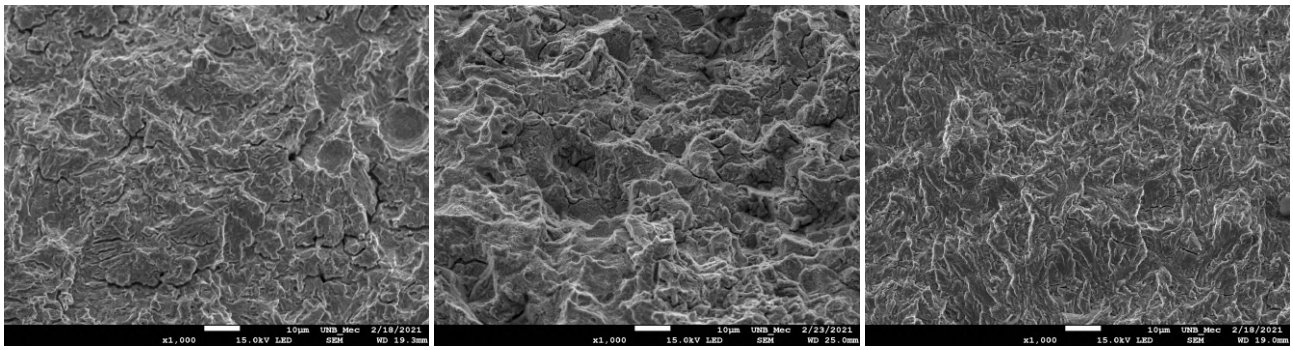

(a) (b) (c)

Figure 9. Fractured surface morphology for the corrosion-fatigue specimens under (a) SWT = 650 MPa and (b) SWT = 250 MPa. In-air fatigue specimen under (c) SWT = 500 MPa.

Two distinctive behaviours were identified on the fractured surface of the corrosion-fatigue specimens. For higher stress amplitude, Fig. 9a, transgranular failure was observed. This morphology is similar to the one observed in the in-air condition (Fig. 9c). However, for the corrosion-fatigue specimen under lower stress amplitude, Fig. 9b, a portion of intergranular failure was identified. This behaviour was also reported by Zhao *et al.* (2017) for a high strength steel under corrosion-fatigue in maritime environment.

This behaviour suggests that the corrosion-fatigue behaviour of the grade R4 steel can be described in two regimes.

For higher stress amplitudes, a transgranular crack initiation and propagation is observed which suggests a mechanically driven failure. For lower stress amplitudes, the crack boundaries of the material are prone to attack by the corrosive environment, which can cause intergranular crack initiation and a portion of intergranular failure during the propagation phase. This phenomenon can only occur because of the dissolution caused by the corrosive environment. Therefore, this type of failure can be assumed to be electrochemically driven.

4. CONCLUSIONS

A combined effect between mechanical loads and electrochemical responses was observed for corrosion-fatigue of a grade R4 steel in 3.5% wt. NaCl solution. Based on this study, the following conclusions can be drawn:

- For steel under uniaxial cyclic loading, the corrosive environment significantly reduces the material lifetime before failure; a decrease in the corrosion-fatigue life when compared to fatigue in air was observed even for immersion periods as short as 15 h. For longer exposure times the corrosion-fatigue life can be up to two orders of magnitude shorter.
- The mean stress causes a reduction of the observed life for both environmental conditions tested. The Smith-Watson-Topper parameter has shown to be a good option to take the load ratio into account.
- The fraction of the corroded area has a positive correlation with the applied mechanical stress amplitude up to *SWT* = 350 MPa. After this value the corrosion degradation occurs primarily inside the nucleated cracks.
- For the corrosion-fatigue tests, lower mechanical amplitudes causes intergranular failure while the higher amplitudes causes transgranular failure.

5. ACKNOWLEDGEMENTS

This research was partially funded by Petrogal S.A./ISPG Brasil S.A. (contract number GALP 09: Durabilidade de Componentes de Sistemas de Amarração para Uso em Águas Profundas: Experimentação e Modelagem—DSAM) and Agência Nacional do Petróleo, Gás Natural e Biocombustiveis—ANP (Contract number 19103-1). Edgar Mamiya also like to acknowledge the support from the Brazilian Council for Scientific and Technological Development—CNPq (Contracts 310063/2018-3) and from Fundação de Apoio a Pesquisa do Distrito Federal (Contract 0193.001522/2016). The authors thank FCT, through IDMEC, under LAETA project UIDB/50022/2020 and through CQE (UIDB/00100/2020). This study was financed in part by the Coordenação de Aperfeiçoamento de Pessoal de Nível Superior – Brasil (CAPES) – Finance Code 001.

6. REFERENCES

API-2SK, 2018. "Design and analysis of stationkeeping systems for floating structures - 4th edition".

ASTM E 466, 2002. "Standard practice for conducting force controlled constant amplitude axial fatigue tests of metallic materials". Standard, American Society for Testing and Materials, West Conshohocken, PA 19428-2959, United States.

ASTM F 1801, 2004. "Standard practice for corrosion fatigue testing of metallic implant materials". Standard, American Society for Testing and Materials, West Conshohocken, PA 19428-2959, United States.

Canut, F.A., Simões, A.M., Reis, L., Freitas, M., Bastos, I.N., Castro, F.C. and Mamiya, E.N., 2019. "Monitoring of corrosion-fatigue degradation of grade r4 steel using an electrochemical-mechanical combined approach". *Fatigue & Fracture of Engineering Materials & Structures*, Vol. 42, No. 11, pp. 2509–2519. doi:10.1111/ffe.13079. URL https://doi.org/10.1111/ffe.13079.

Fernández, J., Storesund, W. and Navas, J., 2014. "Fatigue performance of grade r4 and r5 mooring chains in seawater". In *Volume 1A: Offshore Technology*. ASME. doi:10.1115/omae2014-23491. URL https://doi.org/10.1115/omae2014-23491.

Fontaine, E., Potts, A., tung Ma, K., Arredondo, A. and Melchers, R.E., 2012. "SCORCH JIP: Examination and testing of severely-corroded mooring chains from west africa". In *Offshore Technology Conference*. Offshore Technology Conference. doi:10.4043/23012-ms. URL https://doi.org/10.4043/23012-ms.

Gabetta, G., 1982. "A METHOD TO MEASURE ELECTROCHEMICAL POTENTIAL AT THE TIP OF a GROWING CRACK DURING AN ENVIRONMENTAL FATIGUE TEST". *Fatigue & Fracture of Engineering Materials and Structures*, Vol. 5, No. 3, pp. 215–220. doi:10.1111/j.1460-2695.1982.tb01248.x. URL https://doi.org/10.1111/j.1460-2695.1982.tb01248.x.

Gordon, R.B., Brown, M.G. and Allen, E.M., 2014. "Mooring integrity management: A state-of-the-art review". In *Offshore Technology Conference*. Offshore Technology Conference. doi:10.4043/25134-ms. URL https://doi.org/10.4043/25134-ms.

HSE, 2006. "Floating production system jip fps mooring integrity. research report 444 prepared for the health and safety executive".

IACS, 2016. "Offshore mooring chain". Standard, International Association Classification Societies.

Larrosa, N.O., Akid, R. and Ainsworth, R.A., 2017. "Corrosion-fatigue: a review of damage tolerance models". *International Materials Reviews*, Vol. 63, No. 5, pp. 283–308. doi:10.1080/09506608.2017.1375644. URL https://doi.org/10.1080/09506608.2017.1375644.

Ma, K.T., Shu, H., Smedley, P., L'Hostis, D. and Duggal, A., 2013. "A historical review on integrity issues of permanent mooring systems". In *Offshore Technology Conference*. Offshore Technology Conference. doi:10.4043/24025-ms. URL https://doi.org/10.4043/24025-ms.

Mamiya, E., Castro, F., Ferreira, G., Filho, E.N., Canut, F., Neves, R. and Malcher, L., 2019. "Fatigue of mooring chain links subjected to out-of-plane bending: Experiments and modeling". *Engineering Failure Analysis*, Vol. 100, pp. 206 – 213. ISSN 1350-6307.

Morgantini, M., MacKenzie, D., Comlekci, T. and van Rijswick, R., 2018. "The effect of mean stress on corrosion fatigue life". *Procedia Engineering*, Vol. 213, pp. 581–588. doi:10.1016/j.proeng.2018.02.053. URL https://doi.org/10.1016/j.proeng.2018.02.053.

Nevshupa, R., Martinez, I., Ramos, S. and Arredondo, A., 2018. "The effect of environmental variables on early corrosion of high–strength low–alloy mooring steel immersed in seawater". *Marine Structures*, Vol. 60, pp. 226–240. doi:10.1016/j.marstruc.2018.04.003. URL https://doi.org/10.1016/j.marstruc.2018.04.003.

Palin-Luc, T., Pérez-Mora, R., Bathias, C., Domínguez, G., Paris, P.C. and Arana, J.L., 2010. "Fatigue crack initiation and growth on a steel in the very high cycle regime with sea water corrosion". *Engineering Fracture Mechanics*, Vol. 77, No. 11, pp. 1953–1962. doi:10.1016/j.engfracmech.2010.02.015. URL https://doi.org/10.1016/j.engfracmech.2010.02.015.

Pérez-Mora, R., Palin-Luc, T., Bathias, C. and Paris, P.C., 2015. "Very high cycle fatigue of a high strength steel under sea water corrosion: A strong corrosion and mechanical damage coupling". *International Journal of Fatigue*, Vol. 74, pp. 156–165. doi:10.1016/j.ijfatigue.2015.01.004. URL https://doi.org/10.1016/j.ijfatigue.2015.01.004.

Rampi, L. and Vargas, P., 2011. *Methodology to account for corrosive environment on accelerated fatigue test on mooring chains within the chain out of plane bending (OPB) fatigue Joint Industry Project (JIP). Fatigue design 2011 : Recueil de conférences proceedings*. CETIM. ISBN 2854009460.

Smith, K., Watson, P. and Topper, T., 1970. "A stress-strain function for the fatigue of metals". *Journal of Materials*, Vol. 5, No. 4, pp. 767–778.

Zhao, T., Liu, Z., Du, C., Dai, C., Li, X. and Zhang, B., 2017. "Corrosion fatigue crack initiation and initial propagation mechanism of e690 steel in simulated seawater". *Materials Science and Engineering: A*, Vol. 708, pp. 181–192. doi:10.1016/j.msea.2017.09.078. URL https://doi.org/10.1016/j.msea.2017.09.078.

7. RESPONSIBILITY NOTICE

The authors are solely responsible for the printed material included in this paper.